Supporting Information

Johnstone and Mantua 10.1073/pnas.1318371111

SI Text

Climate Dataset Comparison for the Northeast Pacific, 1900–2012. ***Sea surface temperature.*** Primary sea surface temperature (SST) data for this study come from the 2°-gridded National Oceanic and Atmospheric Administration (NOAA) Extended Reconstruction SST (ERSST) dataset, version 3b (1). ERSST is a fully interpolated dataset based on uninterpolated International Comprehensive Ocean-Atmosphere Data Set (ICOADS) 2°-gridded measurements from ships, buoys, and other marine platforms (2). ERSST infilling is based on empirical orthogonal function (EOF) methods for high-frequency variations and spatial interpolation for low-frequency (decadal and longer) variations.

SST variability in this study focuses on the leading northeast (NE) Pacific EOF (SST1) time series and variability within an area termed the NE Pacific Arc, defined by the region where local correlations with the SST1 monthly index exceed 0.6 (Fig. 1*A*). The underlying ICOADS data have undergone quality control, but aside from the 2° gridding, have not been spatially interpolated. ICOADS data therefore closely reflect direct observations and provide the basis for most long-term gridded SST products. Fig. S2 illustrates ICOADS data completeness for several time periods, revealing highest data availability along major shipping routes over the global oceans. Since the start of the 20th century, ship-based sampling has covered major branches of the NE Pacific Arc along the US Pacific coast and between the mainland United States, Hawaii, and Asia. Interpolated data products are thus expected to be generally well constrained by observations in this area.

Additional SST datasets obtained for comparison are the uninterpolated 2° ICOADS (version 2.5), the 5° HadSST3 (3) product, the fully interpolated 1° HadISST dataset (4), and 0.5° gridded estimates of temperatures at 5-m depth from the Simple Ocean Data Assimilation (SODA) reanalysis version 2.2.4 (5). All datasets were examined over the 1900–2012 period except SODA, which terminates in 2008.

For comparison of Arc-averaged indices, SST values were initially converted to monthly normalized anomalies, relative to a 1981–2010 baseline (1981–2008 for SODA). Monthly anomalies were then regridded onto the ERSST 2° mesh by linear interpolation, and the gridpoints defining the Arc in ERSST were used to compute monthly area-averaged regional time series. For illustration, these series were converted to annual (July–June) means and renormalized over the 1951–2010 period.

The annual Arc-averaged time series from each dataset displays a similar pattern of variability (Fig. S3*A*), particularly after the early 1940s. All cross-correlations exceed 0.9, and similarly steep warming trends are evident from 1910–1920 to 1940. ERSST estimates are slightly higher than the others during the 1930s and 1940s. The low-frequency differences among the datasets are more clearly seen in the plot of 11-y running means (Fig. S3*B*). ICOADS displays slightly lower anomalies than the others before 1930, when the greatest spread in low-frequency estimates is apparent. In the 11-y averages, peak values of each index occur in the early 1990s, slightly exceeding levels reached around 1940.

The primary differences among the SST datasets concern details in the shape of the strong warming trend from 1920 to 1940. Each dataset, however, shows clear evidence of this trend, and the decadal anomalies converge by 1942. Only small differences are observed among the Arc SST indices after World War II.

Sea-level pressure. The primary National Center for Atmospheric Research (NCAR) 5° sea-level pressure (SLP) dataset (6) has been used in a number of studies to document long-term circulation changes over the Northern Hemisphere and North Pacific (7–10). The NCAR SLP analysis was developed from a variety of sources, with data before 1940 originating primarily from 3- and 6-h weather map analyses archived at the National Climatic Data Center (11). The original authors (6) issued cautions on the reliability of these data before 1922 and recommended comparison with independent datasets in climate change studies, which we have done in this study. NCAR monthly SLP fields are 99.8% complete over the NE Pacific study domain (60°N–20°N, 180°W–100°W). The few missing data were filled with estimates from the most strongly correlated grid box series. Analysis is based primarily on the leading NE Pacific EOF (SLP1), which reflects coherent SLP variations over the region, oriented to match SST, with positive values reflecting negative SLP anomalies. Charts depicting SLP1 are illustrated in this manner; however, variability is discussed in physical terms of SLP anomalies.

As represented by the primary NCAR dataset, notable features of NE Pacific SLP variability include a period of unusually high pressure from 1908 to 1922 and a strong trend toward lower pressure from 1910–1920 to 1940. These features are apparent, although less prominently, in the North Pacific Index (NPI), also from NCAR SLP, which reflects variability in the central North Pacific (65°N–30°N, 160°E–140°W; Fig. 1*D*).

The NE Pacific SLP index derived from NCAR SLP was compared with indices produced from four other sources: ICOADS version 2.5 (2), HadSLP2 (12), the 20th Century Reanalysis version 2 (20CR) (13), and the National Centers for Environmental Prediction-NCAR Reanalysis (NNR) (14). SLP data from ICOADS, like SST, reflect uninterpolated marine observations, primarily from ships. HadSLP2 consists of globally complete 5°-gridded values calculated by optimal interpolation of ICOADS and station records. HadSLP2 data from 1900 to 2004 were merged with the real-time, variance-reduced HadSLP2r dataset to form a complete record from 1900 to 2012. 20CR SLP contains 2°-gridded fields, averaged from an ensemble of numerical weather model simulations that assimilate data from ICOADS and land station SLP records. SLP data from the 2.5°-gridded NNR are commonly used in analyses of recent regional variability and are included here primarily as a modern reference, beginning in 1950.

For direct comparison, each SLP dataset was mapped onto a common 2.5° grid corresponding to the NNR, using the methods described above for SST. Area-averaged SLP anomalies were computed for the region defined by the central NE Pacific area above 20°N where the regridded NCAR SLP correlations with the SLP1 time series are less than −0.6 (Fig. 1*C*).

A comparison of the NE Pacific July–June normalized annual time series from each SLP dataset is illustrated in Fig. S3*C*, and 11-y running means are shown in Fig. S3*D*. All SLP datasets generally agree back to about 1940 (all cross-correlations > 0.9), but substantial discrepancies are apparent in earlier years. Each dataset displays evidence of SLP decline from ~1920 to 1940; however, the onset and magnitude of each trend vary considerably. NCAR and ICOADS display the strongest changes, with SLP falling from strongly positive anomalies around 1920, whereas 20CR and HadSLP2 display values at this time that are closer to the 1951–2010 means.

Before 1920, there are large differences among the low-frequency NE Pacific anomalies in the different SLP datasets. The NCAR index displays persistently positive SLP anomalies back to 1900, whereas the others depart strongly from NCAR and from each other, showing a wide range of positive and negative anomalies.

A number of prior studies have established that North Pacific SLP anomalies are strongly associated with temperatures along North American coast on interannual to multidecadal time scales (9, 15–19). NE Pacific SLP indices from the different datasets were correlated against coastal temperatures to assess the reliability of each over several time periods, including those encompassing the early 20th century. Temperature indices include SST_{ARC} (derived from ERSST) and surface air temperatures $(SAT)_{ARC}$, as well as another index, termed SST_5, consisting of the mean Arc-averaged SST anomaly computed from all five SST datasets compared above. Correlations were computed over the periods 1951–2012, 1921–2012, 1901–2012, 1901–1950, and 1901–1920 from annual time series and also detrended series, calculated separately for each interval (Table S1).

Over 1951–2012 and 1921–2012, the different SLP datasets, using both trended and detrended series, correlate similarly with temperature, consistent with their generally similar variability. Nearly all SLP correlations with Arc SST fall in the range of 0.6–0.75, whereas those with SAT_{ARC} are lower by ~0.1.

These SLP–temperature relationships establish a basis for testing the fidelity of each SLP product in the earliest part of the 20th century, when the records strongly diverge. Correlations that include the 1901–1920 interval (1901–1920, 1901–1950, and 1901–2012) are consistently highest with the NCAR dataset, using both trended and detrended indices, suggesting that it provides the most reliable representation of early 20th century conditions. NCAR SLP, unlike the other datasets, depicts historically high SLP over the NE Pacific before 1921 (Fig. S3*B*), a period when it outperforms the other datasets. Positive NCAR SLP anomalies before 1921 are consistent with the general negative correlation between NE Pacific SLP and coastal SST on shorter time scales.

High SLP from 1900 to 1920 in the north-central Pacific, as reflected in the NPI, is consistent with persistently negative anomalies in the Alaska–Japan winter precipitation difference and a number of tropical climate anomalies (although not eastern tropical Pacific SST) (7) (Fig. 1*B*). NE Pacific SLP1 does not correlate strongly with precipitation over land. ICOADS winds were also examined but were judged to be unsuitable for analysis due large nonclimatic inhomogeneities (20).

1. Smith TM, Reynolds RW, Peterson TC, Lawrimore J (2008) Improvements to NOAA's historical merged land-ocean surface temperature analysis (1880-2006). *J Clim* 21(10):2283–2296.
2. Woodruff SD, et al. (2011) ICOADS Release 2.5: Extensions and enhancements to the surface marine meteorological archive. *Int J Climatol* 31(7):951–967.
3. Kennedy JJ, Rayner NA, Smith RO, Parker DE, Saunby M (2011) Reassessing biases and other uncertainties in sea surface temperature observations measured in situ since 1850: 1. Measurement and sampling uncertainties. *J Geophys Res Atmos* 116:D14103.
4. Rayner NA, et al. (2003) Global analyses of sea surface temperature, sea ice, and night marine air temperature since the late nineteenth century. *J Geophys Res Atmos* 108(D14):4407.
5. Carton JA, Giese BS (2008) A reanalysis of ocean climate using Simple Ocean Data Assimilation (SODA). *Mon Weather Rev* 136(8):2999–3017.
6. Trenberth KE, Paolino JA (1980) The Northern Hemisphere sea-level pressure data set: Trends, errors and discontinuities. *Mon Weather Rev* 108(7):855–872.
7. Deser C, Phillips AS, Hurrell JW (2004) Pacific interdecadal climate variability: Linkages between the tropics and the North Pacific during boreal winter since 1900. *J Clim* 17(16):3109–3124.
8. Mantua NJ, Hare SR, Zhang Y, Wallace JM, Francis RC (1997) A Pacific interdecadal climate oscillation with impacts on salmon production. *Bull Am Meteorol Soc* 78(6):1069–1079.
9. Trenberth KE (1990) Recent observed interdecadal climate changes in the Northern Hemisphere. *Bull Am Meteorol Soc* 71(7):988–993.
10. Trenberth KE, Paolino DA (1981) Characteristic patterns of variability of sea level pressure in the Northern Hemisphere. *Mon Weather Rev* 109(6):1169–1189.
11. Hurrell J, Trenberth K, Staff NCAR (2013) The Climate Data Guide: NCAR Sea Level Pressure. Available at: https://climatedataguide.ucar.edu/climate-data/ncar-sea-level-pressure. Accessed July 17, 2014.
12. Allan R, Ansell T (2006) A new globally complete monthly historical gridded mean sea level pressure dataset (HadSLP2): 1850-2004. *J Clim* 19(22):5816–5842.
13. Compo GP, et al. (2011) The twentieth century reanalysis project. *Q J R Meteorol Soc* 137(654):1–28.
14. Kalnay E, et al. (1996) The NCEP/NCAR 40-year reanalysis project. *Bull Am Meteorol Soc* 77(3):437–471.
15. Cayan DR (1992) Latent and sensible heat flux anomalies over the northern oceans: Driving the sea surface temperature. *J Phys Oceanogr* 22(8):859–881.
16. Cayan DR (1992) Latent and sensible heat flux anomalies over the northern oceans: The connection to monthly atmospheric circulation. *J Clim* 5(4):354–369.
17. Chhak KC, Di Lorenzo E, Schneider N, Cummins PF (2009) Forcing of low-frequency ocean variability in the northeast Pacific. *J Clim* 22(5):1255–1276.
18. Schneider N, Cornuelle BD (2005) The forcing of the Pacific Decadal Oscillation. *J Clim* 18(21):4355–4373.
19. Trenberth KE, Hurrell JW (1994) Decadal atmosphere-ocean variations in the Pacific. *Clim Dyn* 9(6):303–319.
20. Cardone VJ, Greenwood JG, Cane MA (1990) On trends in historical marine wind data. *J Clim* 3(1):113–127.

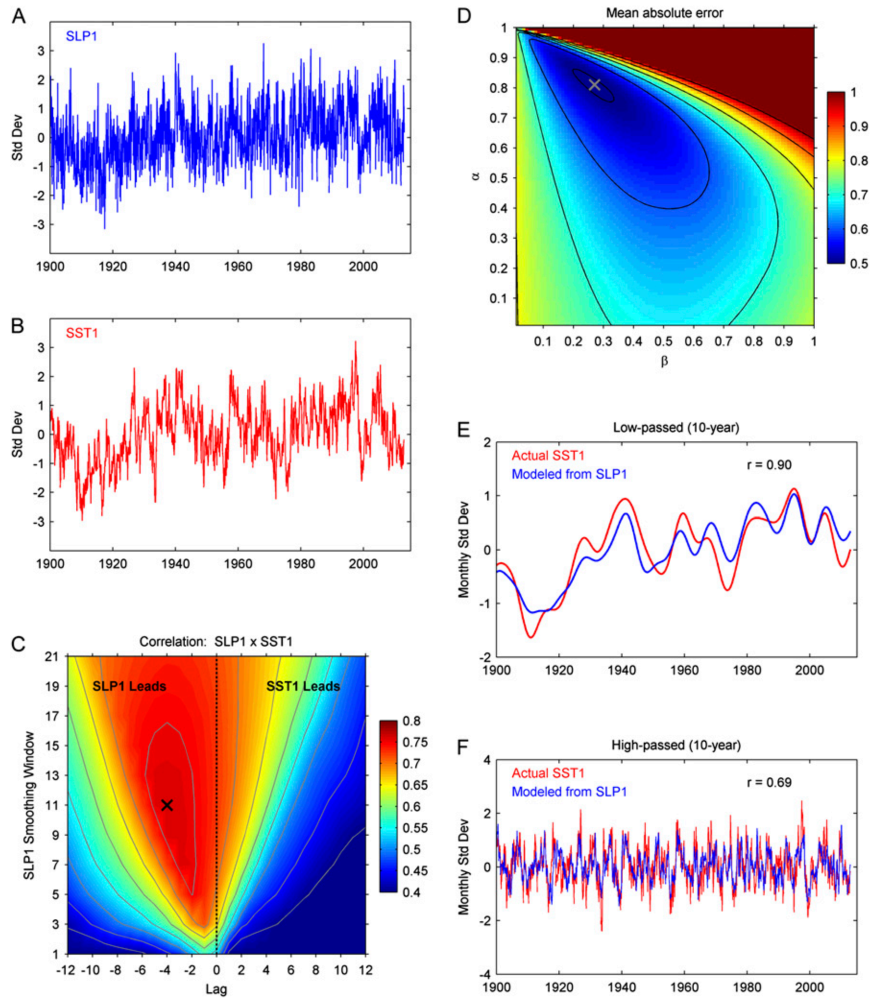

Fig. S1. SLP1-SST1 time series relationships. (*A*) Monthly SLP EOF 1 (SLP1) time series. (*B*) SST EOF1 (SST1) time series. (*C*) Correlations between monthly SST1 and SLP1 plotted by length of smoothing window and lag shift (both in months) applied to SLP1. Contours match tick labels on color scale. X marks maximum correlation of 0.76 with an 11-mo window and SLP1 leading by 4 mo. (*D*) Sensitivity test results of SLP1-SST1 time series model, showing mean absolute errors (in monthly SDs) between modeled and observed SST1 for different combinations of coefficients α (persistence) and β (SLP1 perturbation). X marks the error-minimizing combination: $\alpha = 0.81$, $\beta = 0.27$. (*E*) Comparison of actual and modeled SST1 series after low-pass filtering to retain variations at periods >120 mo. (*F*) Comparison of high-frequency residuals from low-pass filtering.

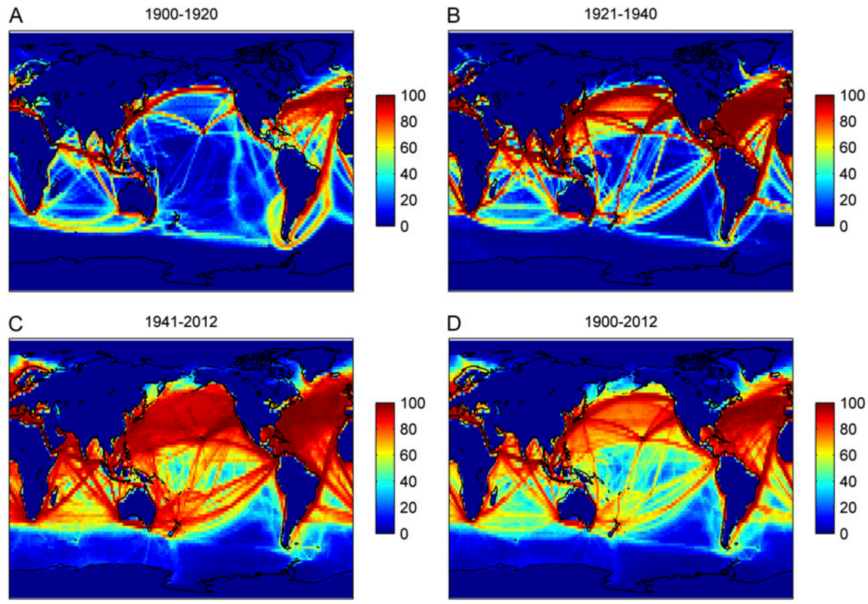

Fig. S2. Percentage of available monthly 2°-gridded observations in ICOADS SST: (*A*) 1900–1920; (*B*) 1921–1940; (*C*) 1941–2012; and (*D*) 1900–2012.

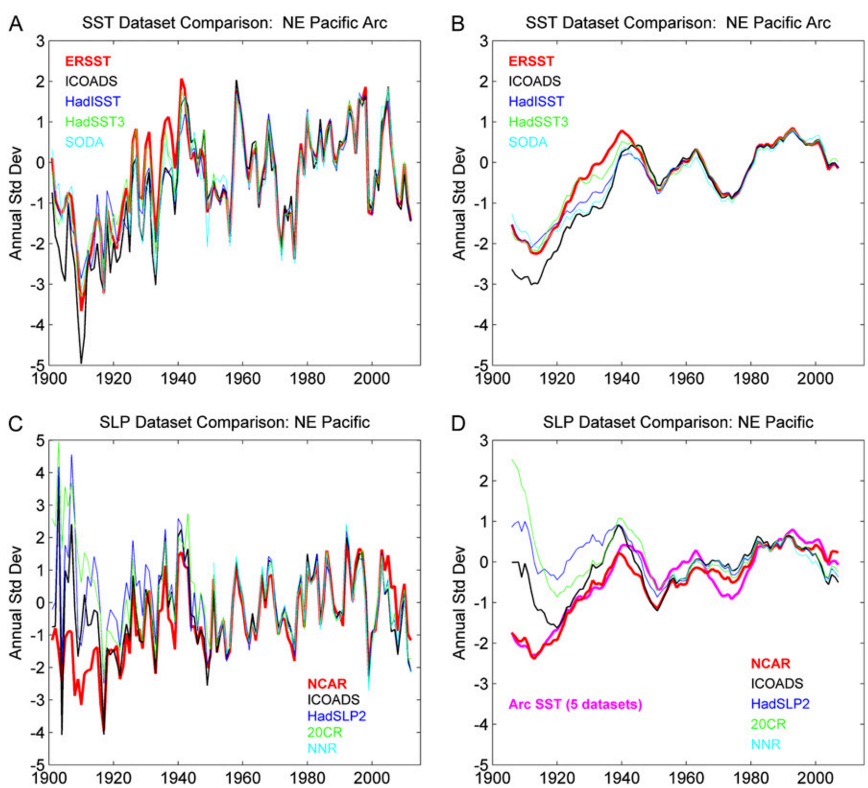

Fig. S3. Dataset comparison for the NE Pacific (*A*) annual (July–June) normalized SST anomalies from each dataset (1951–2012 baseline) over the NE Pacific Arc. (*B*) SST 11-y means. (*C*) Annual central NE Pacific SLP anomalies from each dataset (sign inverted to match SST). (*D*) Eleven-year means, illustrated with SST_5 index (Arc average anomaly from five datasets).

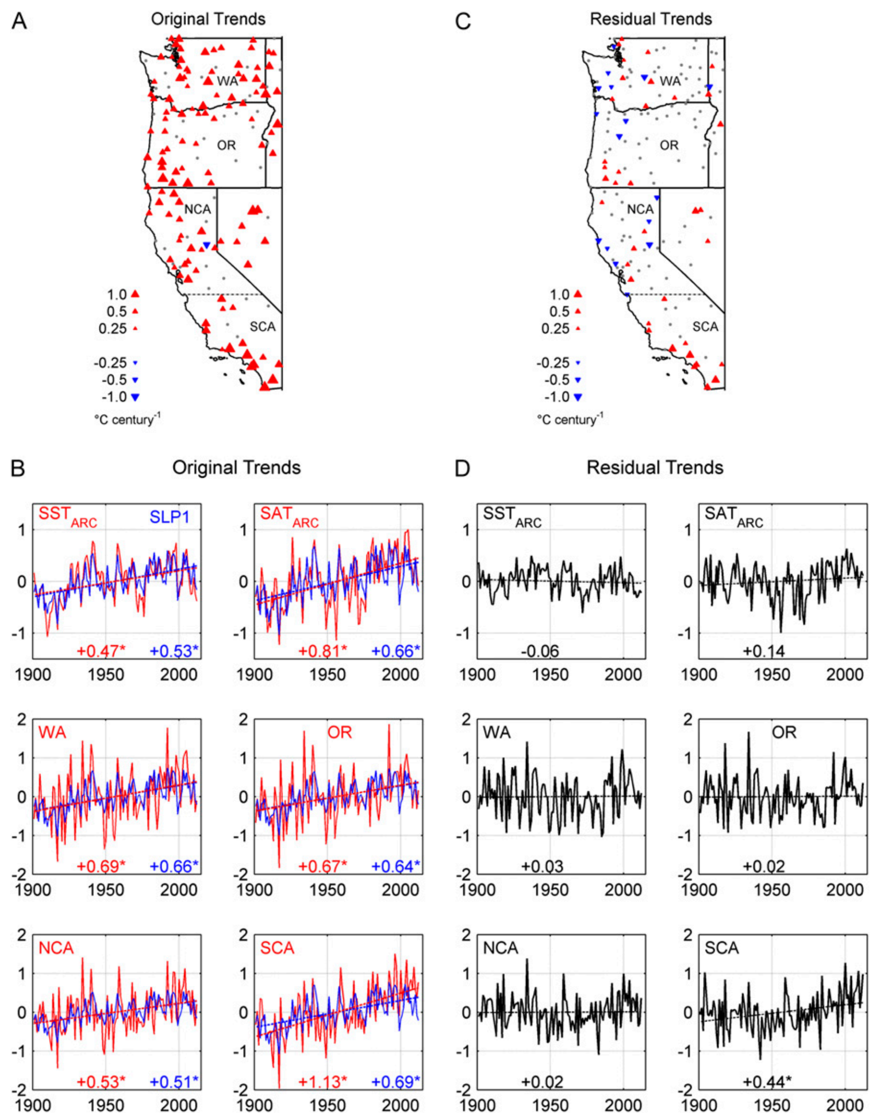

Fig. S4. NE Pacific annual temperature anomalies and trends, 1901–2012. (*A*) Map of trends (°C/century) of annual (July–June) mean SAT for USHCNv2 stations west of 116°W. Triangles mark statistically significant ($P < 0.05$) trends (red, upward pointing: positive; blue, downward pointing: negative). Gray dots mark locations of insignificant trends. (*B*) Red curves, trend lines, and trend values (°C/century) at bottom correspond to annual temperature indices: SST_{ARC}, SAT_{ARC}, and mean USHCNv2 station SAT anomalies for western US states/regions: WA (Washington), OR (Oregon), NCA (northern California), and SCA (southern California). Blue curves, trends, and trend values depict SLP1 temperature signals (scaled copies of SLP1) determined by regressing each annual temperature index on SLP1 and reconstructing the SLP1 component in °C anomalies. (*C*) Map of residual SAT trends after removal of SLP1 temperature signals. (*D*) Same as *B*, for residual temperature indices (blue curves subtracted from red curves). *Statistically significant ($P < 0.05$) trends.

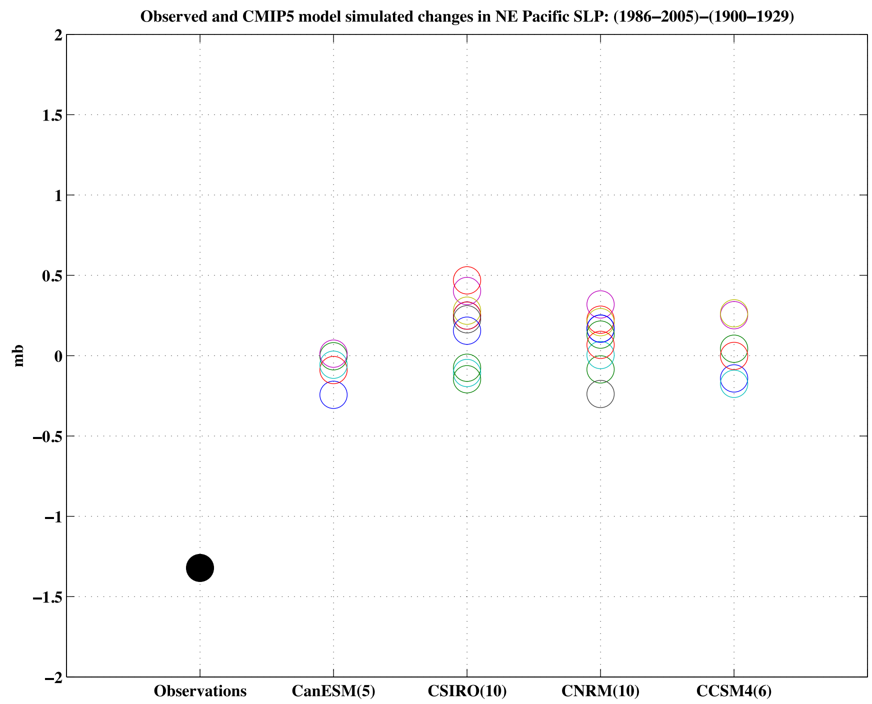

Fig. S5. Observed and CMIP5-simulated changes in July–June annual mean northeast Pacific SLP (177.5E-232.5E, 17.5N-42.5N) (1986–2005) – (1900–1929). Filled black circle indicates the observed SLP change, whereas open circles indicate simulated changes for individual climate model ensemble members. Each of the four different climate models is labeled on the *x* axis, and the number in parentheses indicates the size of the ensemble for each model.

Table S1. Correlations of NE Pacific SLP indices from different datasets with coastal temperature indices

	Trended			Detrended		
Interval, dataset	SST_5	SST_{ARC}	SAT_{ARC}	SST_5	SST_{ARC}	SAT_{ARC}
1951–2012						
NCAR	**0.72**	**0.72**	**0.64**	**0.71**	**0.71**	**0.62**
20CR	0.69	0.71	0.54	0.70	0.71	0.62
HadSLP2	0.69	0.70	0.56	0.70	0.71	0.64
ICOADS	0.68	0.68	0.53	0.68	0.68	0.58
NNR	0.64	0.65	0.48	0.66	0.66	0.58
1921–2012	SST_5	SST_{ARC}	SAT_{ARC}	SST_5	SST_{ARC}	SAT_{ARC}
NCAR	**0.74**	**0.72**	**0.70**	**0.72**	**0.74**	**0.66**
20CR	0.71	0.74	0.62	0.72	0.74	0.64
HadSLP2	0.62	0.70	0.58	0.68	0.72	0.70
ICOADS	0.70	0.73	0.57	0.73	0.73	0.63
1901–2012	SST_5	SST_{ARC}	SAT_{ARC}	SST_5	SST_{ARC}	SAT_{ARC}
NCAR	**0.82**	**0.80**	**0.75**	**0.75**	**0.76**	**0.66**
20CR	0.58	0.61	0.56	0.59	0.61	0.57
HadSLP2	0.39	0.46	0.45	0.56	0.58	0.64
ICOADS	0.27	0.32	0.31	0.50	0.49	0.55
1901–1950	SST_5	SST_{ARC}	SAT_{ARC}	SST_5	SST_{ARC}	SAT_{ARC}
NCAR	**0.83**	**0.85**	**0.80**	**0.78**	**0.81**	**0.78**
20CR	0.49	0.52	0.59	0.58	0.60	0.60
HadSLP2	0.36	0.41	0.57	0.58	0.62	0.65
ICOADS	0.23	0.23	0.36	0.66	0.62	0.55
1901–1920	SST_5	SST_{ARC}	SAT_{ARC}	SST_5	SST_{ARC}	SAT_{ARC}
NCAR	**0.73**	**0.74**	**0.66**	**0.69**	**0.71**	**0.61**
20CR	0.30	0.34	0.39	0.18	0.20	0.29
HadSLP2	0.42	0.47	0.54	0.33	0.37	0.48
ICOADS	0.40	0.48	0.47	0.16	0.22	0.36

Correlations are shown for untreated anomaly series and detrended series, calculated separately for each interval. Correlations from the primary NCAR SLP dataset are in bold text.

Table S2. Cross-correlations among annual (July–June) means of regional climate indices

Variable	Index	SLP						SST					Coastal SAT						State SAT			
		SLP1	*NPI-*	*PNA*	*WPI*	*SOI-*	*AO*	*SST1*	*SST_{ARC}*	*PDO*	*NPGO-*	*Niño 3.4*	*SAT_{ARC}*	*Alaska*	*BC*	*NW US*	*California*	*Hawaii*	*W US*	*WA*	*OR*	*NCA*
SLP	*SLP1*																					
	NPI-	0.70																				
	PNA	0.35	0.68																			
	WPI	−0.11	0.01	−0.02																		
	SOI-	0.49	0.48	0.41	0.27																	
	AO	0.28	0.43	0.39	0.15	0.20																
SST	*SST1*	0.80	0.56	0.37	−0.05	0.42	0.25															
	SST_{ARC}	0.79	0.56	0.37	−0.02	0.43	0.25	0.99														
	PDO	0.43	0.51	0.57	0.01	0.56	0.25	0.57	0.58													
	NPGO-	0.43	0.10	−0.16	0.01	0.39	0.09	0.44	0.45	0.23												
	Niño 3.4	0.61	0.49	0.44	0.31	0.84	0.29	0.54	0.54	0.47	0.30											
Coastal SAT	*SAT_{ARC}*	0.75	0.66	0.59	−0.07	0.49	0.09	0.80	0.80	0.62	0.03	0.60										
	Alaska	0.47	0.57	0.59	−0.02	0.53	0.21	0.60	0.60	0.72	−0.07	0.56	0.84									
	BC	0.63	0.58	0.52	0.10	0.51	0.09	0.73	0.73	0.59	0.10	0.58	0.92	0.81								
	NW US	0.66	0.41	0.33	−0.19	0.11	−0.03	0.66	0.63	0.21	−0.06	0.29	0.69	0.38	0.51							
	CA	0.71	0.64	0.52	0.01	0.50	0.03	0.70	0.71	0.52	0.16	0.59	0.88	0.63	0.80	0.52						
	Hawaii	0.74	0.51	0.45	−0.32	0.25	−0.01	0.70	0.68	0.40	0.02	0.40	0.81	0.47	0.62	0.66	0.76					
State SAT	*W US*	0.65	0.50	0.41	−0.24	0.24	−0.12	0.56	0.56	0.32	−0.02	0.36	0.77	0.41	0.63	0.53	0.87	0.88				
	WA	0.58	0.55	0.43	0.06	0.41	−0.10	0.52	0.52	0.38	0.04	0.50	0.76	0.49	0.70	0.44	0.94	0.65	0.88			
	OR	0.61	0.50	0.36	−0.08	0.28	−0.09	0.50	0.50	0.29	0.03	0.38	0.70	0.36	0.60	0.44	0.89	0.75	0.96	0.94		
	NCA	0.55	0.40	0.29	−0.39	0.11	−0.09	0.48	0.47	0.30	−0.06	0.19	0.63	0.31	0.46	0.44	0.67	0.86	0.92	0.66	0.83	
	SCA	0.63	0.34	0.31	−0.46	0.06	−0.14	0.53	0.51	0.21	−0.09	0.23	0.67	0.31	0.49	0.60	0.62	0.93	0.87	0.57	0.72	0.88

Indices include SLP1 (this study); North Pacific Index (NPI) (1) https://climatedataguide.ucar.edu/sites/default/files/climate_index_files/npindex_monthly_0.txt, Pacific-North American (PNA) index www.cpc.ncep.noaa.gov/products/precip/CWlink/pna/norm.pna.monthly.b5001.current.ascii.table; West Pacific Index ftp://ftp.cpc.ncep.noaa.gov/wd52dg/data/indices/wp_index.tim; Southern Oscillation Index (SOI) www.cgd.ucar.edu/cas/catalog/climind/SOI.signal.ascii; Arctic Oscillation (AO) www.cpc.ncep.noaa.gov/products/precip/CWlink/daily_ao_index/monthly.ao.index.b50.current.ascii; SST1 (this study); SST_{ARC} (this study); Pacific Decadal Oscillation (PDO) http://jisao.washington.edu/pdo/PDO.latest; North Pacific Gyre Oscillation (NPGO) (2) www.o3d.org/npgo/; Niño 3.4 SST (5°*N*-5°S, 170°W-120°W) from ERSST; SAT indices were constructed from USHCNv2 (3) and GHCNv3 (4) land stations. All correlations are for 1901–2012, except AO, SOI, PNA, WPI, and NPGO (1951–2012). NPI, SOI, and NPGO indices were inverted to correspond with others.

1. Trenberth KE, Hurrell JW (1994) Decadal atmosphere-ocean variations in the Pacific. *Clim Dyn* 9(6):303–319.
2. Di Lorenzo E, et al. (2008) North Pacific Gyre Oscillation links ocean climate and ecosystem change. *Geophys Res Lett* 35(8):L08607.
3. Menne M J, Williams CN, Vose RS (2009) The United States Historical Climatology Network monthly temperature data: Version 2. *Bull Am Meterol Soc* 90(7):993–1007.
4. Lawrimore JH, et al. (2011) An overview of the Global Historical Climatology Network monthly mean temperature data set, version 3. *J Geophys Res Atmos* 116:D19121.

Table S3. SD of annual mean (July–June) area-averaged NE Pacific sea level pressure (177.5°E–232.5°E, 17.5°N–42.5°N) from CMIP5 preindustrial control and historical period simulations and from observations

Source	Preindustrial control	Historical (1850-2005)	1900–2012
CCSM4	1.02 (500 y)	0.92 (0.84–0.97; 5)	
	0.40	**0.35 (0.28–0.38)**	
CNRM-CM5	0.75 (850 y)	0.76 (0.71–0.81; 10)	
	0.32	**0.31 (0.26–0.36)**	
CSIRO-Mk3-6–0	1.03 (500 y)	1.00 (0.90–1.11; 10)	
	0.41	**0.43 (0.35–0.49)**	
CanESM2	0.87 (996 y)	0.90 (0.85–0.93; 6)	
	0.34	**0.36 (0.33–0.41)**	
Observations			0.90
			0.61

All values are given in hPa. The first number is the mean SD of all ensemble members, and numbers in parentheses in the historical column indicate the range of SDs for different ensemble members, which is followed by the number of ensemble members. Boldface type indicates the SD for 10-y low pass-filtered time series.

Other Supporting Information Files

Dataset S1 (XLSX)